BMP4 inhibits corneal neovascularization by interfering with tip cells in angiogenesis

Weijin Nan
The Second Hospital of Jilin University
Yuxi He
The Second Hospital of Jilin University
Sitong Shen
The Second Hospital of Jilin University
Meiliang Wu
The Second Hospital of Jilin University
Shurong Wang
The Second Hospital of Jilin University
Yan Zhang (ahzhangyolanda@163.com)
Jilin University Second Hospital

Research Article

Keywords: Corneal neovascularization, Bone morphogenetic protein 4, Tip cells, Stalk cells, Inflammation, Neutrophil extracellular traps

Posted Date: April 14th, 2023

DOI: https://doi.org/10.21203/rs.3.rs-2748603/v1

Abstract

Corneal neovascularization (CNV) can lead to impaired corneal transparency, resulting in vision loss or blindness. The primary pathological mechanism underlying CNV is an imbalance between pro-angiogenic and anti-angiogenic factors, with inflammation playing a crucial role. Notably, a vascular endothelial growth factor VEGF -A gradient triggers the selection of single endothelial cells ECs into primary tip cells that guide sprouting, while a dynamic balance between tip and stalk cells maintains a specific ratio to promote CNV. Despite the central importance of tip-stalk cell selection and shuffling, the underlying mechanisms remain poorly understood. In this study, we examined the effects of BMP4 on VEGF-A-induced lumen formation in human umbilical vein endothelial cells (HUVECs) and CD34-stained tip cell formation. In vivo, BMP4 inhibited CNV caused by corneal sutures. This process was achieved by BMP4 decreasing the protein expression of VEGF-A and VEGFR2 in corneal tissue after corneal suture injury. By observing the ultrastructure of the cornea, BMP4 inhibited the sprouting of tip cells and brought forward the appearance of intussusception. Meanwhile, BMP4 attenuated the inflammatory response by inhibiting neutrophil extracellular traps NETs formation through the NADPH oxidase-2 NOX-2 pathway. Our results indicate that BMP4 inhibits the formation of tip cells by reducing the generation of NETs, disrupting the dynamic balance of tip and stalk cells and thereby inhibiting CNV, suggesting that BMP4 may be a potential therapeutic target for CNV.

1 Introduction

In general, the cornea is avascular, transparent, and an essential component of the refractive system (Sharif and Sharif,2019). Corneal neovascularization (CNV) is caused by a variety of reasons, including infection, inflammation, and chemical injury(Nicholas and Mysore,2021). In severe cases, it can damage vision and even lead to blindness(Tang, et al.,2011). Treatments for CNV include topical steroids, non-steroidal anti-inflammatory agents, laser cautery, fine-needle diathermy, amniotic membrane transplantation, anti-vascular endothelial growth factor (VEGF)agents, and even gene therapy(Nicholas and Mysore,2021). However, all of these methods have limits and side effects(Roshandel, et al.,2018). Therefore, an alternative drug is necessary to be found.

The mechanism of inflammation-induced CNV is the imbalance between pro- and anti-angiogenic factors(Chang, et al.,2012). After corneal injury, corneal epithelial and endothelial cells, stromal keratinocytes, and immune cells (such as T cells and macrophages) can release some pro-angiogenic cytokines to activate corneal limbal vascular endothelial cells and promote neovascularization(Philipp, et al.,2000). These vascular endothelial cells release protein hydrolases that degrade the vascular basement membrane and surrounding corneal extracellular matrix, allowing vascular endothelial cells to migrate into the corneal stroma(Conway, et al.,2001). Vascular endothelial cells move toward the site of inflammation through chemotaxis and grow new vascular lumens and associated branches. Tip-stalk cell selection and shuffling are the building blocks of sprouting angiogenesis. VEGF is one of the initiators of angiogenesis. The selection of single endothelial cells to become the leading tip cells that guide emerging sprouts was triggered by gradients of VEGF-A (Gerhardt, et al.,2003). Tip cells are characterized with long

fingerlike protrusions called filopodia which make motile behavior(Blanco and Gerhardt,2013). Stalk cells trail behind the tip cells in the growing sprout. Under right conditions, stalk cells proliferate, elongate the sprouts, form lumens, and build blood circulation. The VEGF-VEGFR-Dll4-Notch pathway is essential in the sprouting of endothelial cells. Endothelial cells that first upregulate VEGFR2 expression gain an advantage in competition with neighboring endothelial cells and transform into tip cells(García-Pascual, et al.,2013). The tip cells exhibited high levels of VEGFR2 and the stalk cells had low levels of VEGFR2. Tip and stalk cells dynamically compete for the position of the tip cell. It has been shown that the RIN2/Rab5C mechanism leads to premature degradation of VEGFR2, which interferes with normal vascular endothelial VEGF/Notch signaling to produce functional tip cells and sprout angiogenesis(Kempers, et al.,2021). A number of factors and signaling pathways have been involved in tip-stalk cell selection and shuffling, but how they affect tip-stalk cell selection and shuffling requires further investigation.

CNV is often accompanied by excessive infiltration of neutrophils(Shang, et al.,2020). Neutrophils induce a disorganized expansion of the inflammatory response and CNV by producing neutrophil extracellular traps (NETs)(Yuan, et al.,2020). NETs are extracellular structures composed of web-like decondensed chromatin fibers and granule proteins bound to them, which can be released by activated neutrophils and used to capture and kill pathogens(Jorch and Kubes,2017). Notably, NETs play a pro-angiogenic role in a variety of disease processes. NETs exacerbate the inflammatory response and angiogenesis in corneal alkali burn models(Yuan, et al.,2020). NETs can also induce pulmonary hypertension by inducing proliferation and outgrowth of human pulmonary artery endothelial cells and increasing their expression of pro-angiogenic factors(Aldabbous, et al.,2016). Therefore, it is essential to control the rational production of NETs.

Increasing evidence supports the role of bone morphogenetic proteins (BMPs) in intravascular homeostasis and angiogenesis. In laser-induced choroidal neovascularization model, up-regulated BMP4 could inhibit the expression of MMP-9 and VEGF(Xu, et al.,2012). BMP4 decreased VEGF expression in vivo through tsp1-dependent(Tsuchida, et al.,2014). BMP2 and BMP6 synergistically modulated VEGF-induced endothelial cell sprouting via regulating VEGFR, Notch or TAZ-Hippo signaling(Pulkkinen, et al.,2021). In addition, knockdown of BMP4 in adipocytes resulted in increased production of pro-inflammatory cytokines, including tumor necrosis factor α (TNFα), interleukin 1β (IL-1β), interleukin 6 (IL-6) and C–C motif chemokine ligand 2 (CCL2/MCP1)(Mu, et al.,2021). BMP4 may also alleviate nonalcoholic steatohepatitis by inhibiting hepatic ferroptosis(Wang, et al.,2022). Our group's previous experiments have demonstrated that BMP4 can inhibit CNV in the process of repairing corneal injury(Hu, et al.,2021). In this study, we proved that BMP4 could inhibit CNV by interfering with tip cells in angiogenesis and by reducing NETs. Therefore, BMP4 is expected to be an effective drug for the treatment of CNV.

2 Materials And Methods

2.1 Cell culture

The human umbilical vein endothelial cells (HUVECs) were purchased from Shanghai Zhong Qiao Xin Zhou Biotechnology Co.,Ltd. After recovery, HUVECs were cultured in endothelial cell medium (ECM,Sciencell) under conditions of 5% CO_2 and 37°C incubator.

2.2 CNV Model

Seven -to eight-week-old wistar rats (female, 200-220g) were purchased from Liaoning Changsheng biotechnology Co.,Ltd. for experiments. Wistar rats were randomly grouped, 6 rats per group. The study was approved by the Ethics Committee of Jilin University. The animal experiment strictly adhered to the Guide for the Care and Use of Laboratory Animals published by the National Institutes of Health.

The suture method was used to induce rat CNV. Rats were anesthetized by intraperitoneal injection with pentobarbital (30 ~ 50 mg/kg). Under the operating microscope, the surgeon firstly positioned the cornea with a 4mm corneal trephine, then inserted a nylon 10 − 0 shovel needle about 1.5 mm from the limbus of cornea and sutured the cornea at 4 o'clock ,8 o'clock and 12 o'clock. The nylon 10 − 0 shovel needle were used to penetrate the deep corneal stroma without penetrating the endothelium as a stimulus to induce CNV. After modeling, we dropped 20 μg/ ml BMP4(R&D)to left eyes as BMP4 group and reconstitution buffer 4 0.1% Bovine Serum Albumin in 4 mM HCl, R&D to right eyes as solvent control group, 5 μl per time, three times a day for 3,5 or 7 days. In addition, there was a suture group (no drug after modeling) for 3,5 or 7 days, and an untreated group (no suture, no drug).

To investigate the role of Noxs in suture-induced CNV, the Nox inhibitor diphenyleneiodonium chloride (DPI)(Sigma-Aldrich, St. Louis, MO, USA was used in eye drops. The DPI stock solution was prepared in DMSO at a concentration of 3 Mm and diluted to 3 μM in PBS for use. The final concentration of DMSO in each eye drop was less than 0.1%. DPI eye drops were given immediately after corneal injury, four times daily for 7 days. Saline with an equivalent concentration of DMSO was used as the control.

For the rat model, all our procedures followed the Association for Research in Vision and Ophthalmology (ARVO) Statement for the Use of Animals in Ophthalmic and Vision Research.

2.3 Cell viability assay

Cell viability was analyzed by the CCK-8 assay kit. In brief, cells were plated in 96-well culture plates ($7x10^3$ cells/well) in seven groups. The cells were cultured at 37˚C and 5% CO2 for 24 h, then starved for 8h, and 100μl volume of different concentrations of VEGF-A in ECM (0.5%FBS) were added. The final concentrations of VEGF-A were 0,2,5,10,20,50 and 100ng/ml. The cells were washed once with PBS following culture for 24 h, and were then incubated with serum-free ECM with 10 μl CCK-8 solution for 2 h. The OD 450 nm absorbance was measured using a microplate spectrophotometer.

2.4 Tube formation assay

An aliquot of matrigel (Corning) was warmed up at room temperature and then left on ice briefly. Matrigel was plated into each well (100 μl/well) on 96-well culture plates and incubated for 1 hour at 37°C until adequate polymerization. Next,$1×10^4$ HUVECs were co-cultured in basal medium alone, with 20ng/ml

VEGF-A(ECM)or with 20ng/ml VEGF-A plus BMP4 20μg/ml ECM for 24h and incubated at 37°C.Tube formation was observed for 24h, and micrographs of co-cultures were captured using microscope.

2.5 Biomicroscopy examination

The induction of CNV was evaluated by biomicroscopy examination at days 3, 5, 7 after the surgical intervention. Corneal analysis was performed with clinical photographs taken by slit lamp biomicroscope. The degree of CNV was determined according to the length, density, area and number of bifurcation points of the neovascularization.

2.6 Hematoxylin and eosin staining

Six corneas from each group were stained with hematoxylin eosin (H&E). The cornea of rats was sclerosed soaking in 4% paraforma-ldehyde for 12h. Paraffin sections were stained by immunohistochemistry (Department of nephrology, the Second Hospital of Jilin University) and images were collected under microscope.

2.7 Transmission electron microscope (TEM)

Six fresh corneas of the rats were fixed in 2.5% glutaraldehyde fixative at 4°C for 4h and processed for electron microscopy(Department of nephrology, the Second Hospital of Jilin University) to observe corneal tissue changes.

2.8 Western blot

The cornea was crushed with liquid nitrogen, then crushed with an ultrasonic comminuter, and then centrifuged for protein extraction. Lysate protein of ten micrograms was separated by SDS-PAGE gel and then transferred to PVDF membrane. The membrane was blocked with 5% non-fat dry milk for 1h and incubated with primary antibodies at 4°C overnight. Protein bands were detected by incubation with horseradish peroxidase-conjugated antibodies for 1h and displayed with enhanced chemiluminescence reagent. The VEGF-A (1:1000, dilution) antibody and NOX-2(1:4000, dilution) antibody was purchased from Proteintech. The VEGFR2(1:1000, dilution) and β-actin (1:3000, dilution) antibodies were purchased from ABclonal.

2.9 Immunofluorescence staining

Cells were fixed with 4% paraformaldehyde for 30 min, followed by a blocking and permeabilization step for 1h in PBS with 1% BSA and 0.5% Triton-X. Cells were incubated overnight at 4°C with antibodies directed against CD34 (1:250, abcam). Secondary antibodies were Dylight 488 goat anti- rabbit - IgG(1:500, Abbkine) and Phalloidin-iFluor 555. DAPI was used as a nuclear counterstain. The samples were observed and photographed under a fluorescence microscope.

The rats were sacrificed by intraperitoneal injection of pentobarbital before the eyes were removed for immunofluorescence staining. The eyes were removed 1, 3, 5 and 7 d after dropping and the corneas were removed and immediately frozen in OCT compound. The OCT-embedded slices of the cornea were

prepared at 3 μm thickness for immunofluorescence staining. The corneal sections were fixed in paraformaldehyde for 20 min and washed three times in PBS for 5 min each. After 1h blocking in PBS containing 10% goat serum, 1% bovine serum albumin, and 0.1% Triton-X, immunofluorescence staining was performed with the following primary antibodies: mouse anti-MPO (1:1000, proteintech), rabbit anti-Histone-H3 (1:1000, proteintech). Secondary antibodies included Dylight 488 goat anti-rabbit IgG (1:400, Abbkine) and Cy3 Goat Anti-Mouse IgG (1:400, Abbkine). After washing 3 times with PBS, sections were incubated with mounting medium, antifading (with DAPI). Fluorescent signals were detected under a fluorescent microscope (Olympus, Japan).

2.10 Statistical Analysis

One-way ANOVA was performed to determine statistical significance using GraphPad Prism 9. Values are presented as mean ± SEM. Differences were considered statistically significant at *P* values less than 0.05.

3 Results

3.1 BMP4 inhibits CNV and inflammation

To evaluate the effect of BMP4 on CNV in vivo, we used the suture method to induce rat CNV. Statistical analysis was carried out on the photos taken by the slit lamp. A subsequent time kinetics study performed on day 3, 5, and 7 demonstrated a progressive increase in the percentage of CNV. Compared with the solvent control group and the suture group, the length, area and density of CNV in BMP4 group on day 5 were significantly reduced.(Fig. 1)BMP4 topically administrated inhibited corneal stromal neovessels. HE staining showed smaller lumen in the BMP4 group than in the other two groups. (Fig. 2) In the solvent control group and the suture group, there were a large number of inflammatory cell infiltration in the stromal layer of the cornea. That in the BMP4 group was significantly decreased at 3 days. (Fig. 2)

3.2 BMP4 down-regulates angiogenesis factors—VEGF-A and VEGFR2

VEGF-A and VEGFR2 have been shown to play a critical roles in the regulation of angiogenesis(Gerhardt, et al.,2003; Jakobsson, et al.,2010). We also used the suture method to induce rat CNV. Corneal angiogenic factors were detected after 3 days of modeling. We used western blot to detect the expression of VEGF-A and VEGFR2 in the process of CNV dropped with BMP4, and studied the effect of BMP4 on CNV from the perspective of molecular biology. Western blot analysis showed that corneal suture could induce increased expression of VEGF-A protein and its receptor VEGFR2. At 3 days, the expression of VEGF and VEGFR2 in the BMP4 group was significantly lower than that in the solvent control group and the suture group. (Fig. 3)

3.3 BMP4 inhibits tube formation of vascular endothelial cells

To investigate the role of BMP4 in regulating angiogenesis in vitro, we first determined the optimal concentration of VEGF-A to induce HUVECs proliferation. The results of CCK-8 assay showed that 2 or 5 ng/ml VEGF-A could not significantly promote the proliferation of HUVECs, while 10,20,50 and 100 ng/ml VEGF-A significantly increased the proliferation rate of HUVECs. This indicates that different concentrations of VEGF-A have significant effects on the proliferation of HUVECs. We studied the promotion of HUVECs proliferation by 20, 50 and 100 ng/ml VEGF-A, finding that 20 ng/ml VEGF-A may be the optimal concentration to promote HUVECs proliferation. (Fig. 4)

Tubular formation of endothelial cells is a key step in angiogenesis. We further performed the matrigel angiogenesis essay to evaluate the influence of BMP4 on VEGF-A-induced HUVECs tube formation. In vitro tube formation experiments showed that HUVECs in the control group formed multiple densely arranged luminal structures in each image, while the 20 μg/ml BMP4 group had fewer and more sparsely arranged luminal structures. Statistical analysis showed that the number of lumens and nodes was significantly reduced in the 20 μg/ml BMP4 group compared with the control group(Fig. 4)To conclude, 20 μg/ml BMP4 significantly inhibited the formation of lumen number of HUVECs.

3.4 BMP4 inhibits CNV by interfering with the formation of tip cells

It has been demonstrated that tip cell phenotype and CD34 expression co-occur in endothelial monolayers in vitro(Siemerink, et al.,2012). To investigate the effect of BMP4 on tip cells in angiogenesis, we detected the effect of BMP4 on CD34 expression in VEGF-A-induced HUVECs by immunofluorescence staining. Compared with the control group, the expression of CD34 was significantly reduced in the BMP4 group.(Fig. 5)The morphology of CD34 + tip cells also changed. These results suggest that BMP4 may inhibit angiogenesis by suppressing the generation of tip cells.

3.5 BMP4 inhibits the sprouting of tip cells

To observe the effect of BMP4 on corneal ultrastructure, we used the suture method to induce CNV in rats. Fresh corneas were taken to make electron microscope sections and then photographed and observed with an electron microscope. We found less sprouts of angiogenesis in the BMP4 group compared with the solvent control group, and the angiogenesis in the BMP4 group showed earlier intussusception compared with the solvent control group.(Fig. 6)These results suggest that BMP4 disrupts the sprouting angiogenesis involving tip cells, preventing the process of angiogenesis from proceeding in an orderly manner.

3.6 BMP4 reduces the formation of NETs in the suture-induced CNV model

The regulation of BMP4 on NETs formation in corneal tissues was investigated. Immunofluorescence staining of rat corneas after suturing showed a significant accumulation of the web-like NETs structure

labeled with DNA (blue), MPO (red), and guanosine histone H3 (green) in the corneal stroma over time. (Fig. 7)The corneas of the rats with BMP4 dropping showed less extracellular co-localization of DNA with MPO and citrullinated histone H3. Fig. 7 This suggests that BMP4 could reduce the formation of NETs in the suture-induced CNV model.

3.7 NETs formation via NOX-dependent pathway in the suture-induced CNV model

NETs formation can be divided into NOX - dependent and NOX - independent pathways in line with whether or not they depend on reduced nicotinamide adenine dinucleotide phosphate oxidase(NOX) (Hamam and Palaniyar,2019).The results of immunofluorescence staining of rat cornea showed that a reduction in NETs formation with the NOX inhibitor DPI. Fig. 8 To investigate the possible role of NOX in suture-induced CNV, we examined the expression of NOX isoforms. The results of western blot analysis revealed the upregulation of NOX-2 in the rat corneas following suture-induced CNV, and DPI inhibited NOX-2 expression. Fig. 8 These results suggest that the formation of NETs in suture-induced CNV is achieved through the NOX-2 pathway. More interestingly, the expression of NOX-2 was also decreased in the BMP4 group. Fig. 8 This suggests that BMP4 can inhibit CNV by regulating NOX-2 pathway-mediated NETs formation.

4 Discussion

CNV is a common eye lesion, a major cause of blindness, and one of the most difficult clinical conditions to cure. Therefore, it is very important to inhibit CNV. BMP4 can promote or inhibit angiogenesis depending on the context of cell types and associated microenvironment (Liao, et al.,2017). Our research group previously found that BMP4 significantly inhibited CNV, and topical application of BMP4 increased the expression of endogenous BMP4 and decreased the expression of angiogenic factors (Hu, et al.,2021).However, this was under the condition of 7 days after corneal sutures and 7 days of dropped eye BMP4. In the suture-induced CNV model, blood vessels grew into the cornea as early as day 2 after suture placement(Cursiefen, et al.,2006). Therefore, the study aims to investigate the mechanism and time effect of BMP4 on early CNV.

Our research group's preliminary experiment proved that the optimal concentration of BMP4 on cornea is 20 μg/ml(Hu, et al.,2021).Therefore, we continued to use the suture method to induce rat CNV and chose 20 μg/ml BMP4 for subsequent experiments. We observed the effect of BMP4 on CNV. The length and area of CNV was found to become shorter and smaller at 5 days of eye dropped with BMP4. VEGF-A and VEGFR2 expression decreased at 3 days of eye BMP4 dropped. Vascular sprouting is a key process of angiogenesis and mainly related to the formation of tip and stalk cells(De Bock, et al.,2013). VEGF gradients induce tip cells and promotes the formation of filopodia(Gerhardt, et al.,2003). When VEGF and VEGFR bind, VEGFR autophosphorylation activates downstream signaling pathways, which can induce tip cells migration, tip cells gene expression, and stalk cells proliferation(Liang, et al.,2014). VEGF-A binding with VEGFR2 promotes the expression of Dll4 mainly by activating the mitogen-activated protein

kinase (MAPK)/extracellular regulated protein kinases (ERK) or phosphatidylinositol 3 kinase (PI3K)/protein kinase B (AKT) signaling pathway. High expression of Dll4 in tip cells activates Notch signaling in its neighboring cells (future stalk cells) and inhibits VEGFR2 expression in these cells(Blanco and Gerhardt,2013). Premature degradation of VEGFR2 disrupts normal endothelial vascular endothelial VEGF/Notch signaling and VEGF-dependent gene expression, however, it fails to produce functional tip cells and sprouting angiogenesis(Kempers, et al.,2021). In this study, the number of lumens and nodes was significantly reduced in the BMP4 group compared with the control group. Our group previously validated the role of BMP4/Smad pathway in CNV. Smad1/5 enhances Notch pathway and increases hairy and enhancer of split 1(HES1) expression in vascular endothelial cells (Moya, et al.,2012). Overexpression of HES1 inhibits the migration and angiogenesis of tip cells(Benn, et al.,2017). All these proved that BMP4 inhibited the growth of tip cells, and therefore interfere the dynamic balance between tip cells and stalk cells, which inhibited CNV. However, the mechanisms of BMP4 regulation of VEGF need to be more extensively explored. Rezzola et al. confirmed that BMP4 induces c-Src phosphorylation by interacting with BMPRI-II heterodimer, which in turn activates VEGFR2 and leads to angiogenic response(Rezzola, et al.,2019). This is contrary to our results. It is hypothesized that BMP4 plays different roles in different situations. We will conduct a more in-depth study on the mechanism of BMP4's effect on CNV at a later stage. The sialomucin CD34 is expressed in a small subset of cultured endothelial cells and these cells extend filopodia: a hallmark of tip cells(Siemerink, et al.,2012). In vivo, the absence of CD34 reduced the density of filopodia on retinal endothelial tip cells in neonatal mice, and its expression promoted the formation of pathological and invasive blood vessels during angiogenesis(Siemerink, et al.,2016). In the present study, we investigated endothelial cells expressing CD34 in endothelial monolayers cultured in vitro. We found a significant decrease in CD34 expression in the BMP4 group. Again, the vitro experiments demonstrated that BMP4 inhibited tip cells. In addition, the different mechanisms of angiogenesis are what we need to focus on. Beginning with the canonical sprouting angiogenesis, followed by vasculogenesis and intussusception, and finishing with vasculogenic mimicry. Intussusception occurs after sprouting angiogenesis or vasculogenesis, and it is described as a means of expanding the capillary plexus without the need of a high-metabolic demand(Burri, et al.,2004). Altered hemodynamics, altered pericyte wall stress, and changes in perceived endothelial cell shear stress due to the lack of CD31 and VEGF are some of the possible events for the initiation of intussusception(Djonov and Makanya,2005). In our experiment, there were obvious sprouting of endothelial cells in the solvent control group, whereas that of the BMP4 group were not obvious learning from the photographs taken by transmission electron microscope. And the angiogenesis in the BMP4 group showed earlier intussusception compared with the solvent control group. We considered that BMP4 inhibited the sprouting of endothelial cells, which resulted in the reduction of the area of vascular extension forward. The expression of VEGF-A decreased after 3 days of BMP4 dropped, and the change of shear stress of endothelial cells led to the initiation of intussusception. Earlier intussusception may shorten the process of angiogenesis and thus inhibit CNV(Zuazo-Gaztelu and Casanovas,2018).

We also observed the effect of BMP4 on inflammatory cells in the corneal suture-induced CNV. In the solvent control group and the suture group, there was a large number of inflammatory cell infiltration in

the stromal layer of the cornea, whereas that of the BMP4 group significantly decreased. Inflammation is a key pathological process in the CNV. Inflammatory cells migrating to the cornea can produce angiogenic factors, which contribute to the development of CNV by disrupting the balance between pro- and anti-angiogenic factors(Sharif and Sharif,2019). MMP9 is a key protein in the regulation of corneal inflammatory neovascularization(Ding, et al.,2019). It has been shown that MMP9 may act both upstream and downstream of VEGF during angiogenesis(Chen, et al.,2020). In laser-induced choroidal neovascularization model, up-regulated BMP4 could inhibit MMP-9 expression directly, and VEGF indirectly(Xu, et al.,2012). Myeloperoxidase (MPO) protein, a major component of neutrophil primary granules in cornea lysate(Borregaard and Cowland,1997). MPO was detected 4 hours right after injury, and it peaked at days 1 and 3, then reduced to 17% of the peak level by day 5(Choi, et al.,2017). Shang et al. found that neutrophil depletion with anti-Ly6G antibodies resulted in significant CNV in the non-depleted group(Shang, et al.,2020). And in the neutrophil depletion group, severe corneal necroses were seen. These results suggest that neutrophils play an important role in corneal repair and neovascularization. Activated neutrophils can release NETs. NETs are extracellular reticulation structures that are composed of chromatin released from the nucleus upon stimulation of neutrophils. NETs takes DNA as the framework, embedded with histones and more than 30 primary and secondary granule components(Döring, et al.,2017). It has been shown that NETs generally acts as an antibacterial agent, but excess NETs can cause damage to surrounding tissues either by itself or by increasing pro-inflammatory responses. In corneal infections, neutrophils capture and kill pathogens by releasing NETs(Papayannopoulos,2018), but the typical notion of NETs is that it can induce a disorganized expansion of the inflammatory response, exacerbating tissue damage and inducing inflammatory angiogenesis(Yuan, et al.,2020).Extracellular localization of NETs can be observed in the corneal alkali burn model(Yuan, et al.,2020), which is consistent with our experimental results. Although our experiments used a corneal suture model, both models induce neovascularization with an inflammatory response at the core. And the stimulation of sutures is persistent, which exacerbates the excess formation of NETs. Next, we explore the formation of NETs. Our results showed that the expression of NOX-2 was significantly increased in the suture group, and that the formation of NETs and expression of NOX-2 were reduced after the application of the NADPH oxidase inhibitor DPI. That is to say, the formation of NETs in suture-induced CNV is achieved through a NOX-2-dependent pathway(Chen, et al.,2022). NOX is the main source of ROS(Leto, et al.,2009). There is evidence that NOX-2 can trigger angiogenesis by upregulating VEGF expression(Wang, et al.,2020)， and VEGF can also increase ROS production by activating the catalytic structural domain of NOX-2(Zou, et al.,2019). Thus, there is a complex interplay between ROS and VEGF signaling in angiogenesis. The application of NADPH oxidase inhibitors DPI can effectively reduce suture-induced oxidative stress, attenuate the inflammatory response, reduce NETs formation, and thus inhibit CNV. More interestingly, NOX-2 expression was decreased in the BMP4 group compared with the suture group and the BMP4 solvent group, and the extracellular localization of NETs was also decreased. We consider that BMP4 interferes with the dynamic balance between tip and stalk cells and thus inhibits CNV by reducing the formation of NETs through inhibition of NOX-2 expression. It has been shown that BMP4 binding to BMPR2 induces ICAM-1 expression and neutrophil-endothelial cell adhesion, which promotes neutrophil crossing of the capillary barrier(Wang, et al.,2018). The researchers developed

a new three-cell co-culture model and found that neutrophils significantly induced VEGF-A expression, upregulated MMPs and significantly regulated BMP4(Herath, et al.,2018). The effect of BMP4 on CNV is mediated through the regulation of neutrophils and MMP9. However, there are few studies on the relationship between BMP4 and NETs at present. Our findings provide ideas for further research on the relationship between BMP4, NETs and CNV in the future. At the same time, macrophages also play an important role in corneal neovascularization. Early stage of inflammation, after macrophage recruitment, they can secrete VEGF-A and VEGFR2(Hadrian, et al.,2021). During cerebral angiogenesis, yolk sac-derived macrophages expressing TIE2 and Nrp1 constitute a major population of tissue macrophages that interact with vascular endothelial cells to promote tip cell formation and sprouting to induce downstream vascular anastomosis(Fantin, et al.,2010). However, the molecular mechanisms by which macrophages mediate tissue angiogenesis are not fully understood. We are not sure if BMP4 inhibits tip cell formation through macrophages. This is what we need to explore in the future.

In conclusion, BMP4 significantly inhibits CNV. This is achieved by reducing the formation of NETs, interfering with the dynamic balance between tip cells and stalk cells, and affecting the mechanism of angiogenesis. It provides a new idea for further research on the mechanism of BMP4 on CNV and the mechanism of angiogenesis, which is expected to be a new target for the treatment of CNV.

Abbreviations

CNV
Corneal neovascularization
BMP4
Bone morphogenetic protein 4
NETs
Neutrophil extracellular traps
NOX-2
NADPH oxidase-2
DPI
Diphenyleneiodonium chloride
HUVECs
Human umbilical vein endothelial cells
ECs
Endothelial cells
VEGF
Vascular endothelial growth factor
VEGFR2
Vascular endothelial growth factor receptor 2
DLL4
Delta-like protein 4
Notch

Neurogenic locus notch homolog protein
RIN2
Ras And Rab Interactor 2
MMP9
Matrix metalloproteinase-9
BMPs
Bone morphogenetic proteins
TNFα
Tumor necrosis factorα
IL-1β
Interleukin 1β
IL-6
Interleukin 6
CCL2
C–C motif chemokine ligand 2
ECM
Endothelial cell medium ECM
H&E
Hematoxylin eosin
TEM
Transmission electron microscope
MAPK
Mitogen-activated protein kinase
ERK
Extracellular regulated protein kinases
PI3K
Phosphatidylinositol 3 kinase
AKT
Protein kinase B
HES1
Hairy and enhancer of split 1
ICAM-1
intercellular adhesion molecule-1
TIE2
Recombinant TEK Tyrosine Kinase, Endothelial
Nrp1
Neuropilin-1
MPO
Myeloperoxidase

Declarations

Competing Interests: No conflict of interest exits in the submission of this manuscript, and manuscript is approved by all authors for publication. I would like to declare on behalf of my co-authors that the work described was original research that has not been published previously, and not under consideration for publication elsewhere, in whole or in part.

Acknowledgments: This research was funded by Jilin Provincial Health Science and Technology Capability Improvement Project, China [grant number 2021JC015]; Interdisciplinary Training Program for young teachers and students of Jilin University ,China [grant number 2022-JCXK-28]; The mechanism of inhibiting corneal neovascularization by BMP4, China [grant number 3R2196623429]; Jilin Province young and middle-aged scientific and technological innovation and entrepreneurship outstanding talents (team) project, China [grant number 20230508076RC]; Natural Science Foundation of Jilin Province, China [grant number YDZJ202301ZYTS067].

Ethics approval and consent to participate: The animal study protocol was approved by the Ethics Committee of Jilin University.

Availability of data and materials: All data generated or analysed during this study are included in this published article.

Authors' contributions: Conceptualization, Weijin Nan and Yan Zhang; methodology, Yuxi He; software, Meiliang Wu; validation, Weijin Nan, Sitong Shen and Yan Zhang; formal analysis, Yuxi He; investigation, Shurong Wang; data curation, Meiliang Wu; writing—original draft preparation, Weijin Nan; writing—review and editing, Weijin Nan ,Yan Zhang and Yuxi He; visualization, Weijin Nan; supervision, Yan Zhang; project administration, Shurong Wang; funding acquisition, Yan Zhang. All authors have read and agreed to the published version of the manuscript.

References

1. Aldabbous L, Abdul-Salam V, McKinnon T et al (2016) Neutrophil Extracellular Traps Promote Angiogenesis: Evidence From Vascular Pathology in Pulmonary Hypertension. Arterioscler Thromb Vasc Biol 36(10):2078–2087
2. Benn A, Hiepen C, Osterland M, Schütte C, Zwijsen A, Knaus P (2017) Role of bone morphogenetic proteins in sprouting angiogenesis: differential BMP receptor-dependent signaling pathways balance stalk vs. tip cell competence. FASEB J 31(11):4720–4733
3. Blanco R, Gerhardt H (2013) VEGF and Notch in tip and stalk cell selection. Cold Spring Harb Perspect Med 3(1):a006569
4. Borregaard N, Cowland JB (1997) Granules of the human neutrophilic polymorphonuclear leukocyte. Blood 89(10):3503–3521

5. Burri PH, Hlushchuk R, Djonov V (2004) Intussusceptive angiogenesis: its emergence, its characteristics, and its significance. Dev Dyn 231(3):474–488
6. Chang JH, Garg NK, Lunde E, Han KY, Jain S, Azar DT (2012) Corneal neovascularization: an anti-VEGF therapy review. Surv Ophthalmol 57(5):415–429
7. Chen L, Lin G, Chen K et al (2020) VEGF promotes migration and invasion by regulating EMT and MMPs in nasopharyngeal carcinoma. J Cancer 11(24):7291–7301
8. Chen Y, Hu H, Tan S et al (2022) The role of neutrophil extracellular traps in cancer progression, metastasis and therapy. Exp Hematol Oncol 11(1):99
9. Choi H, Phillips C, Oh JY et al (2017) Comprehensive Modeling of Corneal Alkali Injury in the Rat Eye. Curr Eye Res 42(10):1348–1357
10. Conway EM, Collen D, Carmeliet P (2001) Molecular mechanisms of blood vessel growth. Cardiovasc Res 49(3):507–521
11. Cursiefen C, Maruyama K, Jackson DG, Streilein JW, Kruse FE (2006) Time course of angiogenesis and lymphangiogenesis after brief corneal inflammation. Cornea 25(4):443–447
12. De Bock K, Georgiadou M, Carmeliet P (2013) Role of endothelial cell metabolism in vessel sprouting. Cell Metab 18(5):634–647
13. Ding XW, Sun X, Shen XF et al (2019) Propofol attenuates TNF-α-induced MMP-9 expression in human cerebral microvascular endothelial cells by inhibiting Ca2+/CAMK II/ERK/NF-κB signaling pathway. Acta Pharmacol Sin 40(10):1303–1313
14. Djonov V, Makanya AN (2005) New insights into intussusceptive angiogenesis.EXS.(94):17–33
15. Döring Y, Soehnlein O, Weber C (2017) Neutrophil Extracellular Traps in Atherosclerosis and Atherothrombosis. Circ Res 120(4):736–743
16. Fantin A, Vieira JM, Gestri G et al (2010) Tissue macrophages act as cellular chaperones for vascular anastomosis downstream of VEGF-mediated endothelial tip cell induction. Blood 116(5):829–840
17. García-Pascual CM, Zimmermann RC, Ferrero H et al (2013) Delta-like ligand 4 regulates vascular endothelial growth factor receptor 2-driven luteal angiogenesis through induction of a tip/stalk phenotype in proliferating endothelial cells. Fertil Steril 100(6):1768–76e1
18. Gerhardt H, Golding M, Fruttiger M et al (2003) VEGF guides angiogenic sprouting utilizing endothelial tip cell filopodia. J Cell Biol 161(6):1163–1177
19. Hadrian K, Willenborg S, Bock F, Cursiefen C, Eming SA, Hos D (2021) Macrophage-Mediated Tissue Vascularization: Similarities and Differences Between Cornea and Skin. Front Immunol 12:667830
20. Hamam HJ, Palaniyar N (2019) Post-Translational Modifications in NETosis and NETs-Mediated Diseases.Biomolecules.9(8)
21. Herath T, Larbi A, Teoh SH, Kirkpatrick CJ, Goh BT (2018) Neutrophil-mediated enhancement of angiogenesis and osteogenesis in a novel triple cell co-culture model with endothelial cells and osteoblasts. J Tissue Eng Regen Med 12(2):e1221–e1236

22. Hu H, Wang S, He Y et al (2021) The role of bone morphogenetic protein 4 in corneal injury repair. Exp Eye Res 212:108769
23. Jakobsson L, Franco CA, Bentley K et al (2010) Endothelial cells dynamically compete for the tip cell position during angiogenic sprouting. Nat Cell Biol 12(10):943–953
24. Jorch SK, Kubes P (2017) An emerging role for neutrophil extracellular traps in noninfectious disease. Nat Med 23(3):279–287
25. Kempers L, Wakayama Y, van der Bijl I et al (2021) The endosomal RIN2/Rab5C machinery prevents VEGFR2 degradation to control gene expression and tip cell identity during angiogenesis. Angiogenesis 24(3):695–714
26. Leto TL, Morand S, Hurt D, Ueyama T (2009) Targeting and regulation of reactive oxygen species generation by Nox family NADPH oxidases. Antioxid Redox Signal 11(10):2607–2619
27. Liang X, Xu F, Li X, Ma C, Zhang Y, Xu W (2014) VEGF signal system: the application of antiangiogenesis. Curr Med Chem 21(7):894–910
28. Liao KH, Chang SJ, Chang HC et al (2017) Endothelial angiogenesis is directed by RUNX1T1-regulated VEGFA, BMP4 and TGF-β2 expression. PLoS ONE 12(6):e0179758
29. Moya IM, Umans L, Maas E et al (2012) Stalk cell phenotype depends on integration of Notch and Smad1/5 signaling cascades. Dev Cell 22(3):501–514
30. Mu W, Qian S, Song Y et al (2021) BMP4-mediated browning of perivascular adipose tissue governs an anti-inflammatory program and prevents atherosclerosis. Redox Biol 43:101979
31. Nicholas MP, Mysore N (2021) Corneal neovascularization. Exp Eye Res 202:108363
32. Papayannopoulos V (2018) Neutrophil extracellular traps in immunity and disease. Nat Rev Immunol 18(2):134–147
33. Philipp W, Speicher L, Humpel C (2000) Expression of vascular endothelial growth factor and its receptors in inflamed and vascularized human corneas. Invest Ophthalmol Vis Sci 41(9):2514–2522
34. Pulkkinen HH, Kiema M, Lappalainen JP et al (2021) BMP6/TAZ-Hippo signaling modulates angiogenesis and endothelial cell response to VEGF. Angiogenesis 24(1):129–144
35. Rezzola S, Di Somma M, Corsini M et al (2019) VEGFR2 activation mediates the pro-angiogenic activity of BMP4. Angiogenesis 22(4):521–533
36. Roshandel D, Eslani M, Baradaran-Rafii A et al (2018) Current and emerging therapies for corneal neovascularization. Ocul Surf 16(4):398–414
37. Shang Q, Chu Y, Li Y et al (2020) Adipose-derived mesenchymal stromal cells promote corneal wound healing by accelerating the clearance of neutrophils in cornea. Cell Death Dis 11(8):707
38. Sharif Z, Sharif W (2019) Corneal neovascularization: updates on pathophysiology, investigations & management. Rom J Ophthalmol 63(1):15–22
39. Siemerink MJ, Hughes MR, Dallinga MG et al (2016) CD34 Promotes Pathological Epi-Retinal Neovascularization in a Mouse Model of Oxygen-Induced Retinopathy. PLoS ONE 11(6):e0157902

40. Siemerink MJ, Klaassen I, Vogels IM, Griffioen AW, Van Noorden CJ, Schlingemann RO (2012) CD34 marks angiogenic tip cells in human vascular endothelial cell cultures. Angiogenesis 15(1):151–163
41. Tang Z, Zhang F, Li Y et al (2011) A mouse model of the cornea pocket assay for angiogenesis study. J Vis Exp. (54)
42. Tsuchida R, Osawa T, Wang F et al (2014) BMP4/Thrombospondin-1 loop paracrinically inhibits tumor angiogenesis and suppresses the growth of solid tumors. Oncogene 33(29):3803–3811
43. Wang J, Xu J, Zhao X, Xie W, Wang H, Kong H (2018) Fasudil inhibits neutrophil-endothelial cell interactions by regulating the expressions of GRP78 and BMPR2. Exp Cell Res 365(1):97–105
44. Wang X, Ma B, Wen X et al (2022) Bone morphogenetic protein 4 alleviates nonalcoholic steatohepatitis by inhibiting hepatic ferroptosis. Cell Death Discov 8(1):234
45. Wang Z, Yang J, Qi J, Jin Y, Tong L (2020) Activation of NADPH/ROS pathway contributes to angiogenesis through JNK signaling in brain endothelial cells. Microvasc Res 131:104012
46. Xu J, Zhu D, Sonoda S et al (2012) Over-expression of BMP4 inhibits experimental choroidal neovascularization by modulating VEGF and MMP-9. Angiogenesis 15(2):213–227
47. Yuan K, Zheng J, Huang X et al (2020) Neutrophil extracellular traps promote corneal neovascularization-induced by alkali burn. Int Immunopharmacol 88:106902
48. Zou J, Fei Q, Xiao H et al (2019) VEGF-A promotes angiogenesis after acute myocardial infarction through increasing ROS production and enhancing ER stress-mediated autophagy. J Cell Physiol 234(10):17690–17703
49. Zuazo-Gaztelu I, Casanovas O (2018) Unraveling the Role of Angiogenesis in Cancer Ecosystems. Front Oncol 8:248

Figures

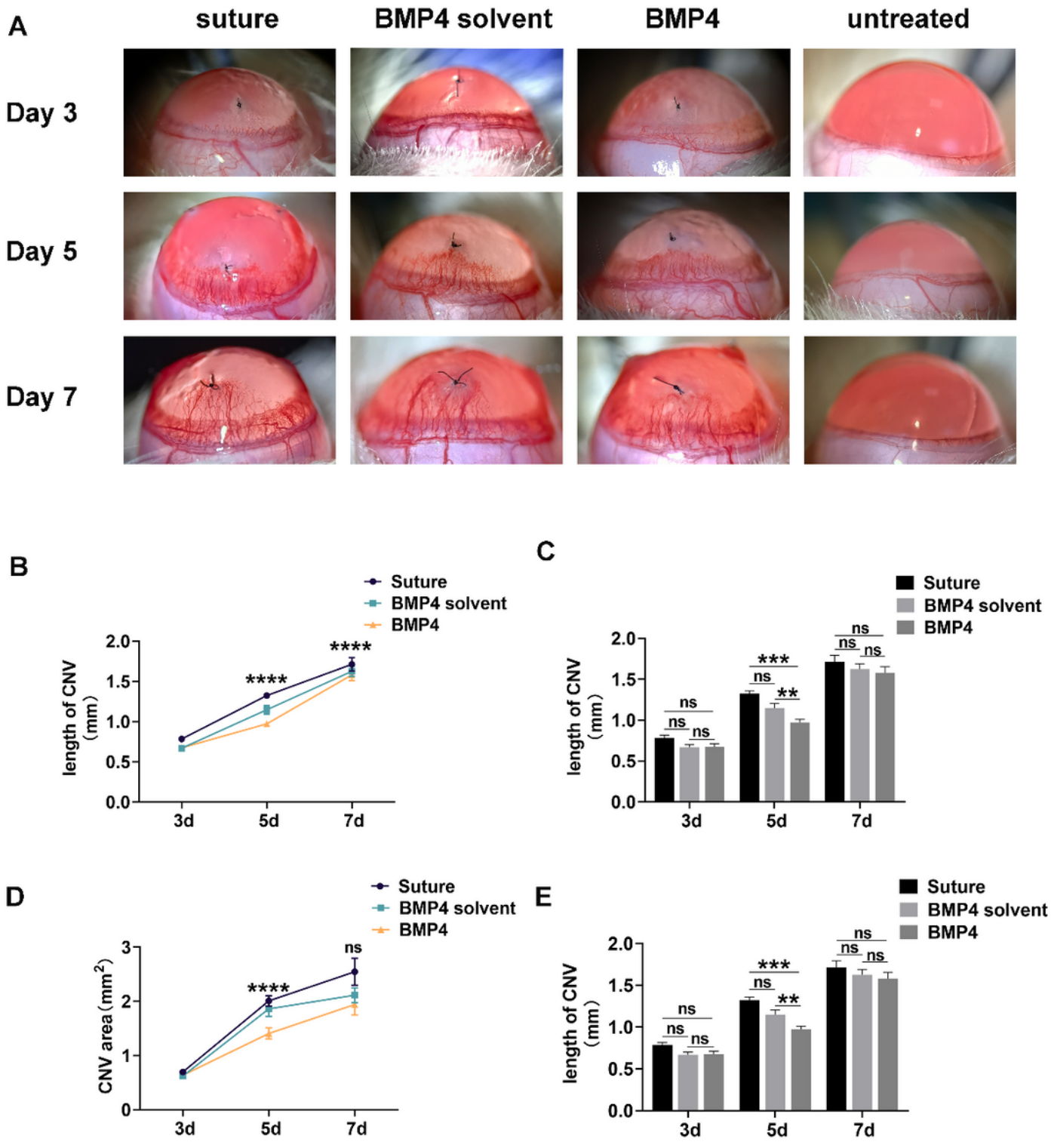

Figure 1

Inhibitory of BMP4 on CNV of rats induced by suture. (A) Slit-lamp microscope photos of rats eyes of the BMP4 group, solvent control group, suture group and the untreated group on days 3,5 and 7. Magnification, x16. (B) Analysis of the length of CNV at 3, 5 and 7 days after suture-induced. (C) A significant regression of the length of CNV was observed in the BMP4 group, compared with the solvent control group and suture group on day 5. (D) Analysis of the CNV area at 3, 5 and 7 days after suture-

induced. (E) A significant regression of the CNV area was observed in the BMP4 group, compared with the solvent control group and suture group on day 5. The length and area of CNV is quantified and normalized(n=6). Results are presented as means±SEM.*P<0.05. **P <0.01.

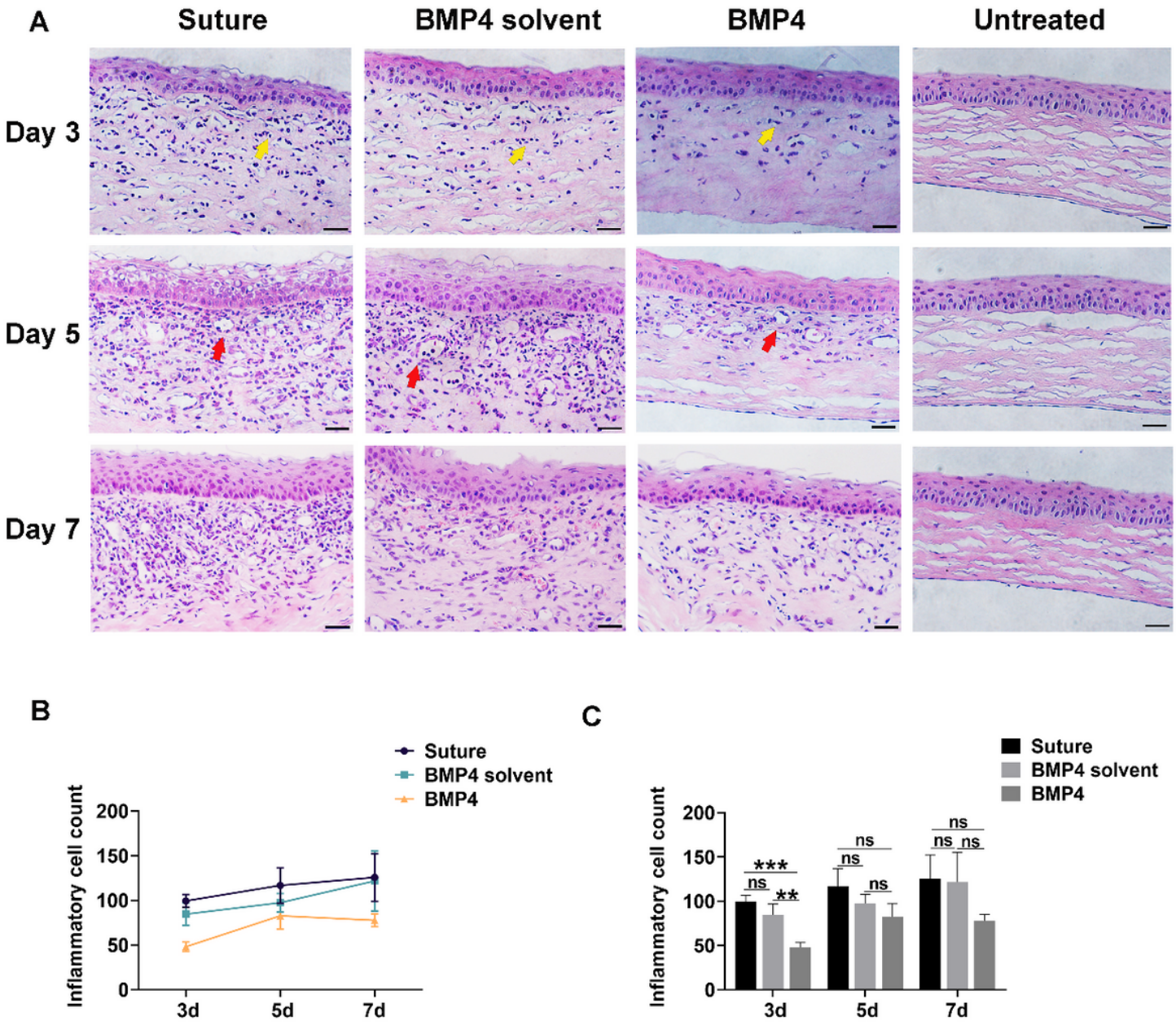

Figure 2

Inhibitory of BMP4 on corneal inflammation of rats induced by suture. (A) HE-stained sections show infiltrating of inflammatory cells on days 3,5 and 7. Inflammatory cells(yellow arrow). Lumen of CNV (red arrow). Scale bars=20μm X400 .(B) Analysis of inflammatory cells numbers at 3, 5 and 7 days after suture-induced. Inflammation cells are included in calculating randomly at least 3fields of each condition. (n=6) (C) A significant regression of the inflammatory cells was observed in the BMP4 group, compared

with the solvent control group and suture group on day 3.Results are presented as means±SEM.**P <0.01.

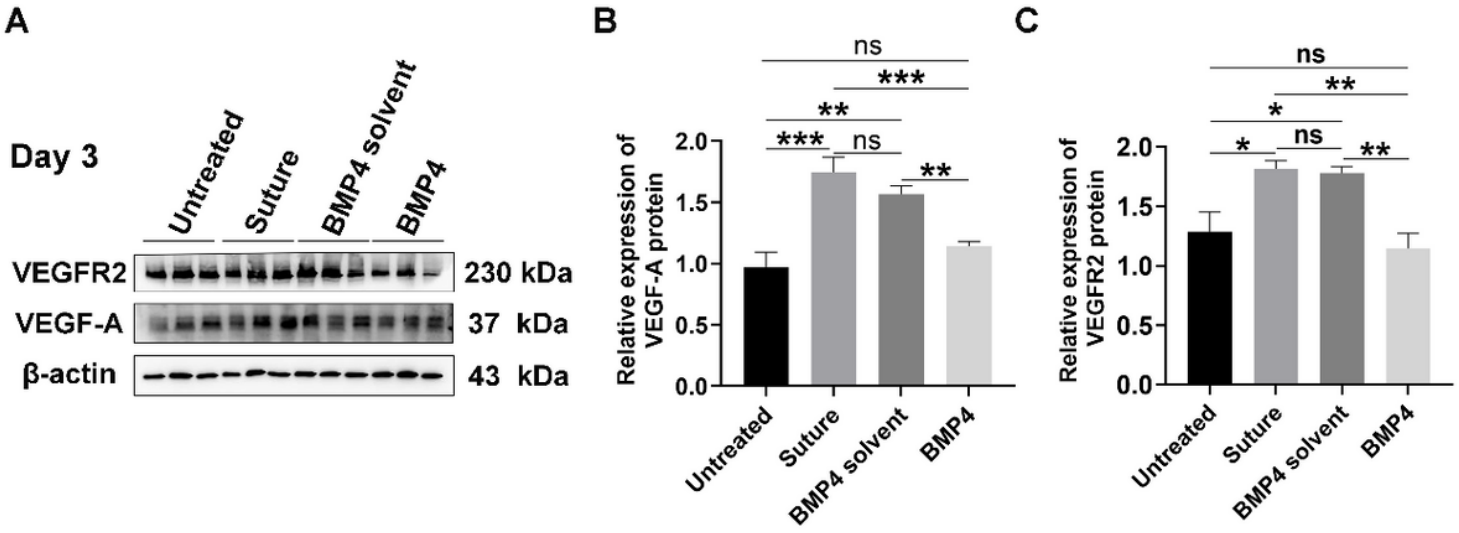

Figure 3

Effect of BMP4 on VEGF-A and VEGFR2 in CNV. (A) Protein expression levels of VEGF-A and VEGFR2 in the BMP4 group, solvent control group, suture group and the untreated group were accessed using western blot analysis on day 3.The three samples of each group presented in western blot bands were different. (B,C) Bands of VEGF-A ,VEGFR2 were quantified using ImageJ software and the data are presented as the mean ± SEM. At 3 days, the expression of VEGF-A and VEGFR2 in the BMP4 group was significantly lower than that in the solvent control group and the suture group.Results are presented as means±SEM. *P<0.05. **P <0.01. (n=6)

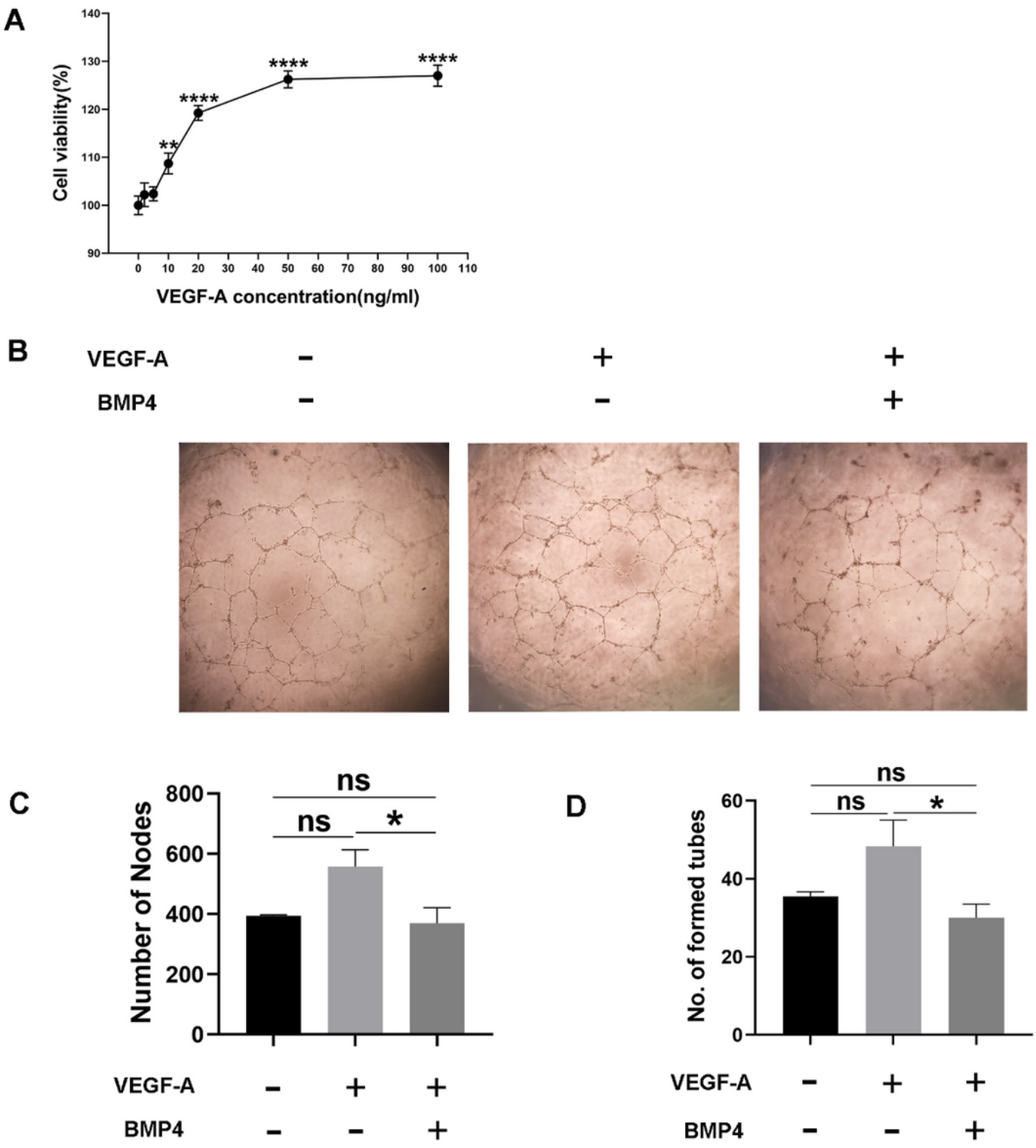

Figure 4

BMP4/VEGF-A interaction is involved in regulating angiogenesis in vitro. (A)The CCK-8 assay was performed to measure the effect of VEGF-A on the viability of HUVECs. (B) Representative brightfield micrographs showing tube formation of HUVECs at 24h of indicated co-cultures. HUVECs were cultured alone in basal media, with VEGF-A supplements or with BMP4 (stimulated with 20 μg/ml for 24 h) at 37°C on a gel matrix to measure tube formation. (C,D) Bar chart showing measures of tube formation

(number of nodes, number of formed tubes).Tube formation was quantified by analyzing brightfield micrographs using Angiogenesis Analyzer plugin in ImageJ software. Data are represented as mean ± SEM. *$p < 0.05$.(n=6)

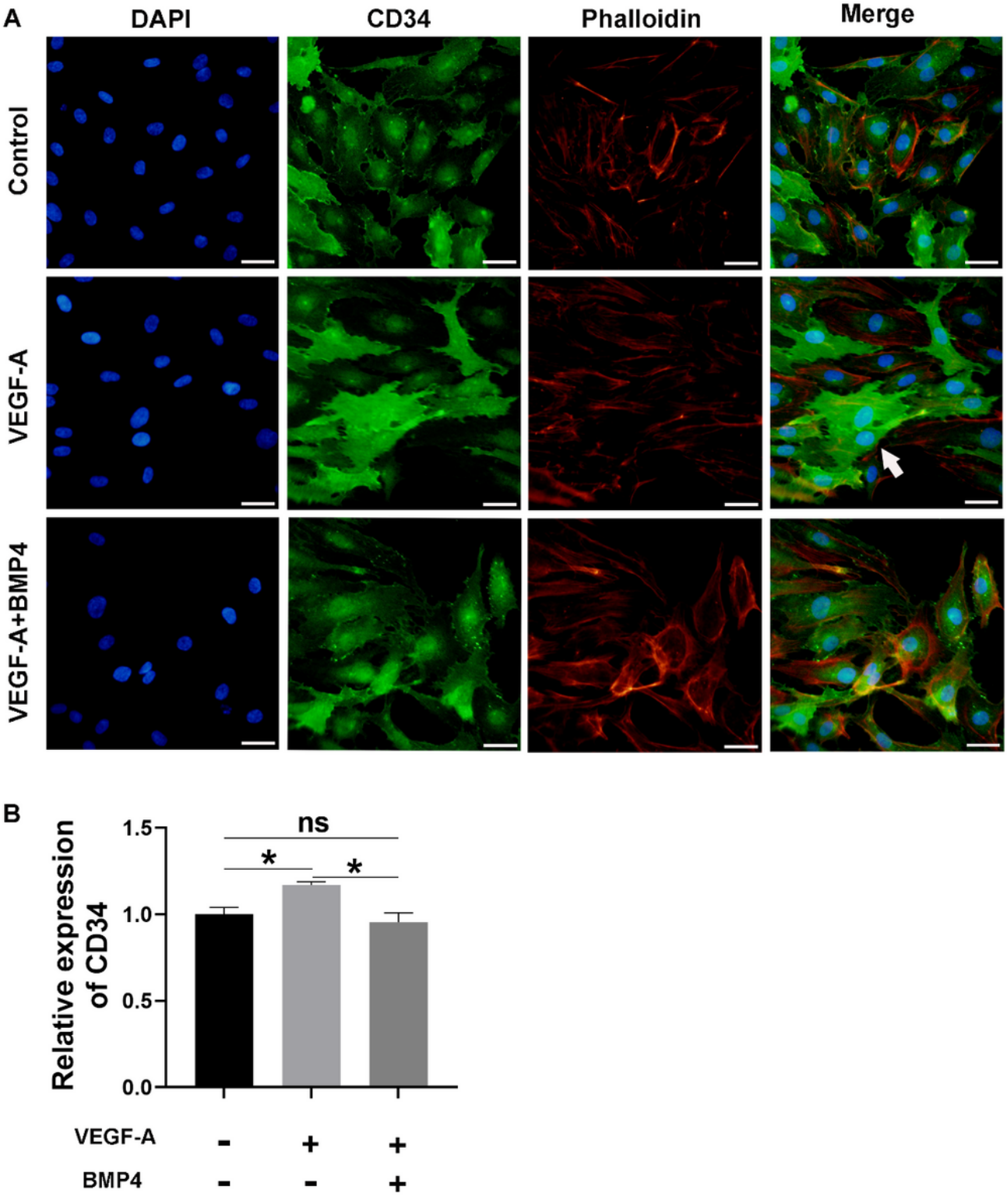

Figure 5

Effects of BMP4 and VEGF-A on CD34+ tip cells. (A) Analysis of $CD34^+$ tip cell morphology. HUVECs were cultured in basal medium alone and co-cultured with VEGF-A or BMP4. Identification of tip cells by staining with anti-CD34 (green), F-actin (phalloidin, red), and nucleus (DAPI, blue) in HUVECs. Arrowheads indicate filopodia-like extrusions on $CD34^+$ cells. Scale bar represents 20 μm. (B)Bars show the relative expression of CD34 of HUVECs treated with VEGF-A or BMP4. Data are represented as mean ± SEM. *p < 0.05. (n=6)

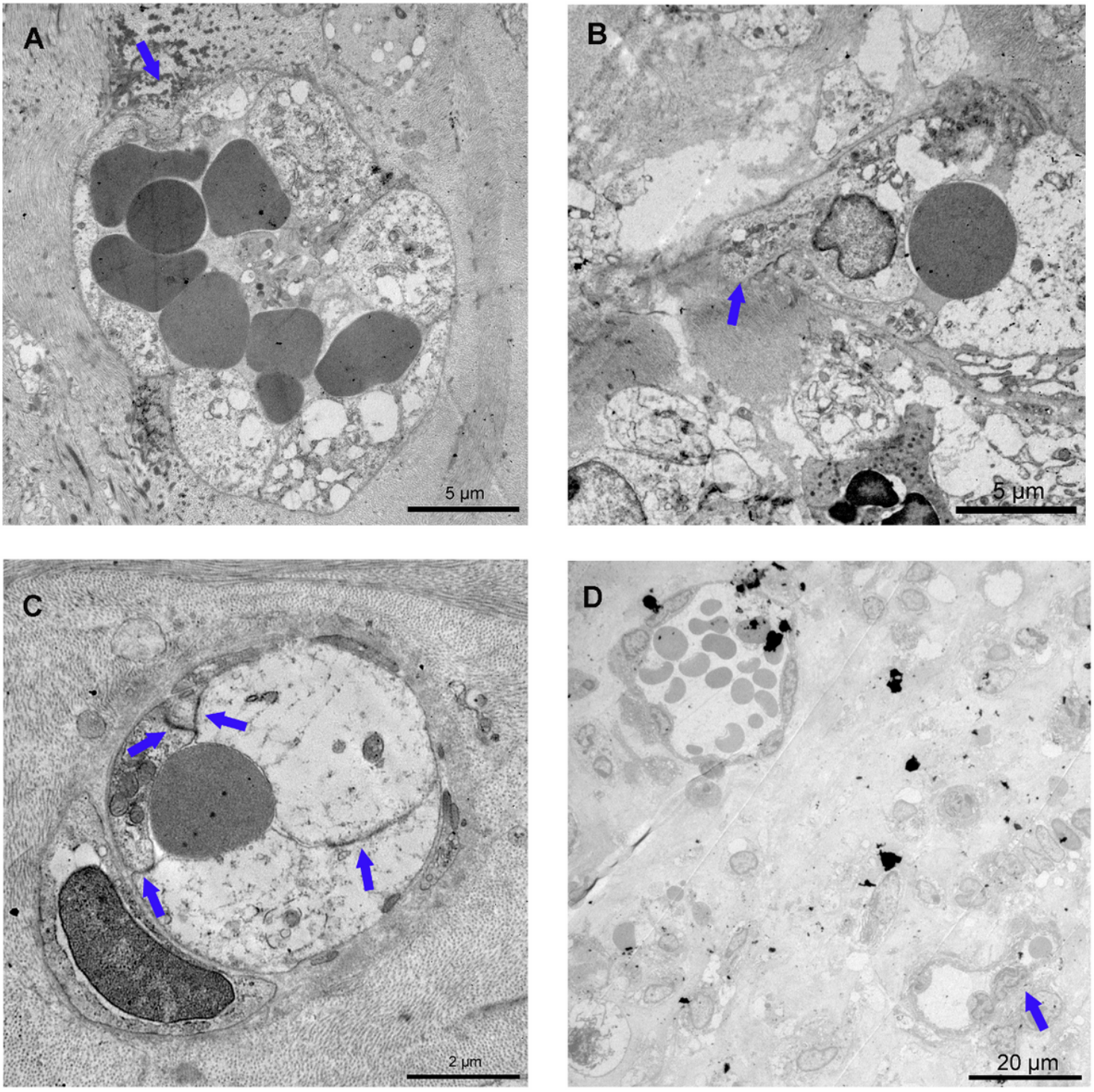

Figure 6

Ultrastructure shows the process of angiogenesis in CNV induced by suture. (A) The solvent control group at 3 days. Multiple irregularly shaped red blood cells (RBCs) and vascular endothelial cells (ECs) are seen in the vessels. The basement membrane at the periphery of the vessel has ruptured, and most of the high electron-density granular debris can be seen at the rupture. The ECs appear to be in a mitotic state and tend to move out of the lumen through the ruptured basement membrane. (The arrow shows). This is the signal of vascular sprouting. (B) The solvent control group at 5 days. The basement membrane at the periphery of the vessel has ruptured. The ECs are in a mitotic state and extend out of the lumen. (The arrow shows). This reflects the characteristic of vascular sprouting. (C) The solvent control group at 7 days. The lumen ECs extend into the lumen and cause slight compression of the RBCs in the blood vessels, causing the RBCs to deform. (The arrow shows). Endothelial cells and blood vessel walls dilated and thickened, and cell connections between endothelial cells increased. This is consistent with the characteristics of intussusception angiogenesis. (D) The BMP4 group at 5 days. The ECs expanded significantly and protrude into the lumen, and the opposite wall collapsed into the lumen accordingly, making the tube walls in relative positions close to each other and bond, and then the blood vessels were radially divided into two independent neovascularization, that is, the process of intussusception angiogenesis was completed. (The arrow shows).

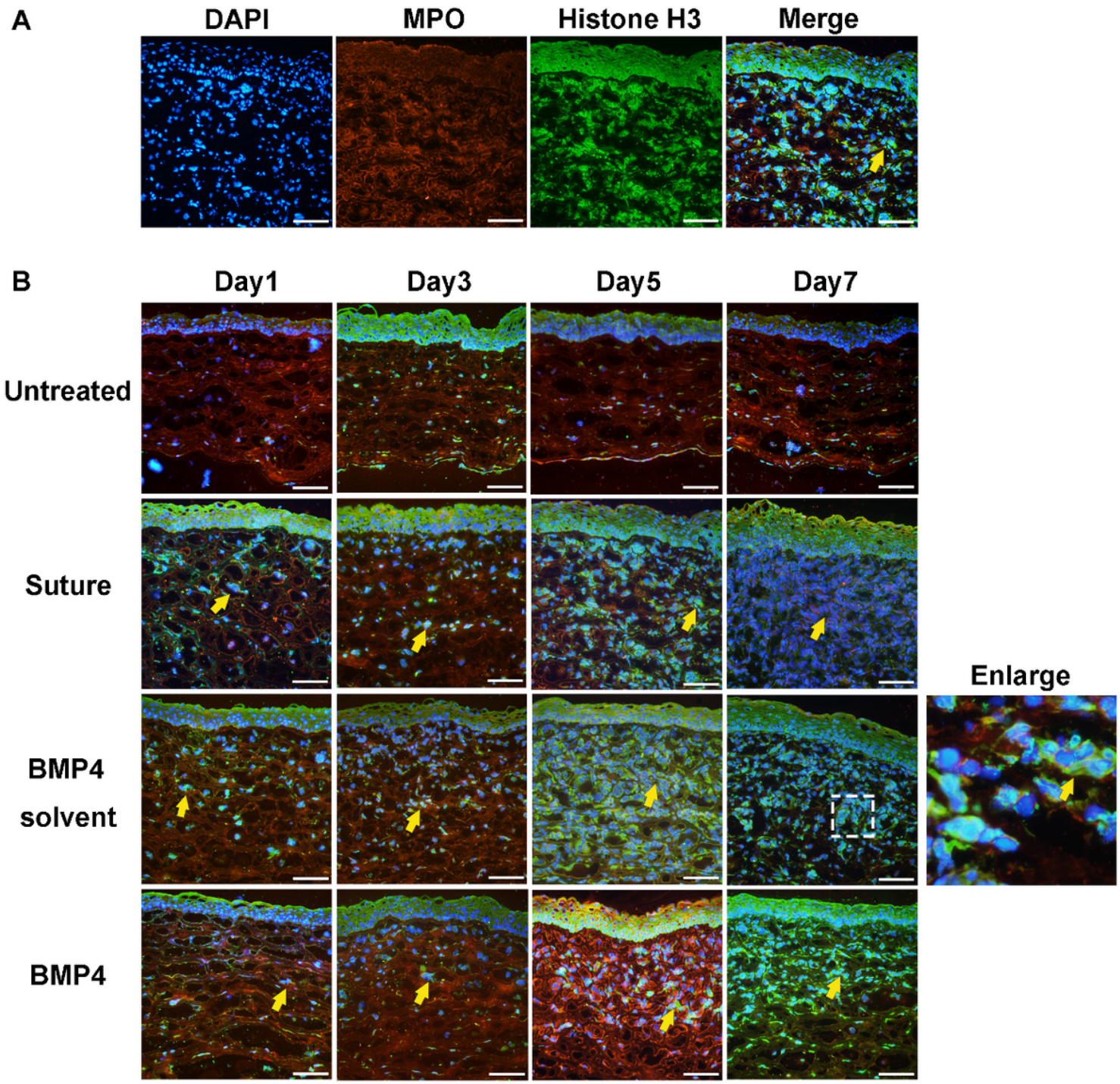

Figure 7

NETs formation was visualized by immunofluorescence staining. (A) Localization of NETs in the cornea. (The arrow shows). (B) In the suture control group, the formation of NETs increased with time. NETs formation was significantly reduced in the BMP4 group compared with the suture group and the solvent control group. Scale bar represents 50 μm. Data are represented as mean ± SEM. (n=6)

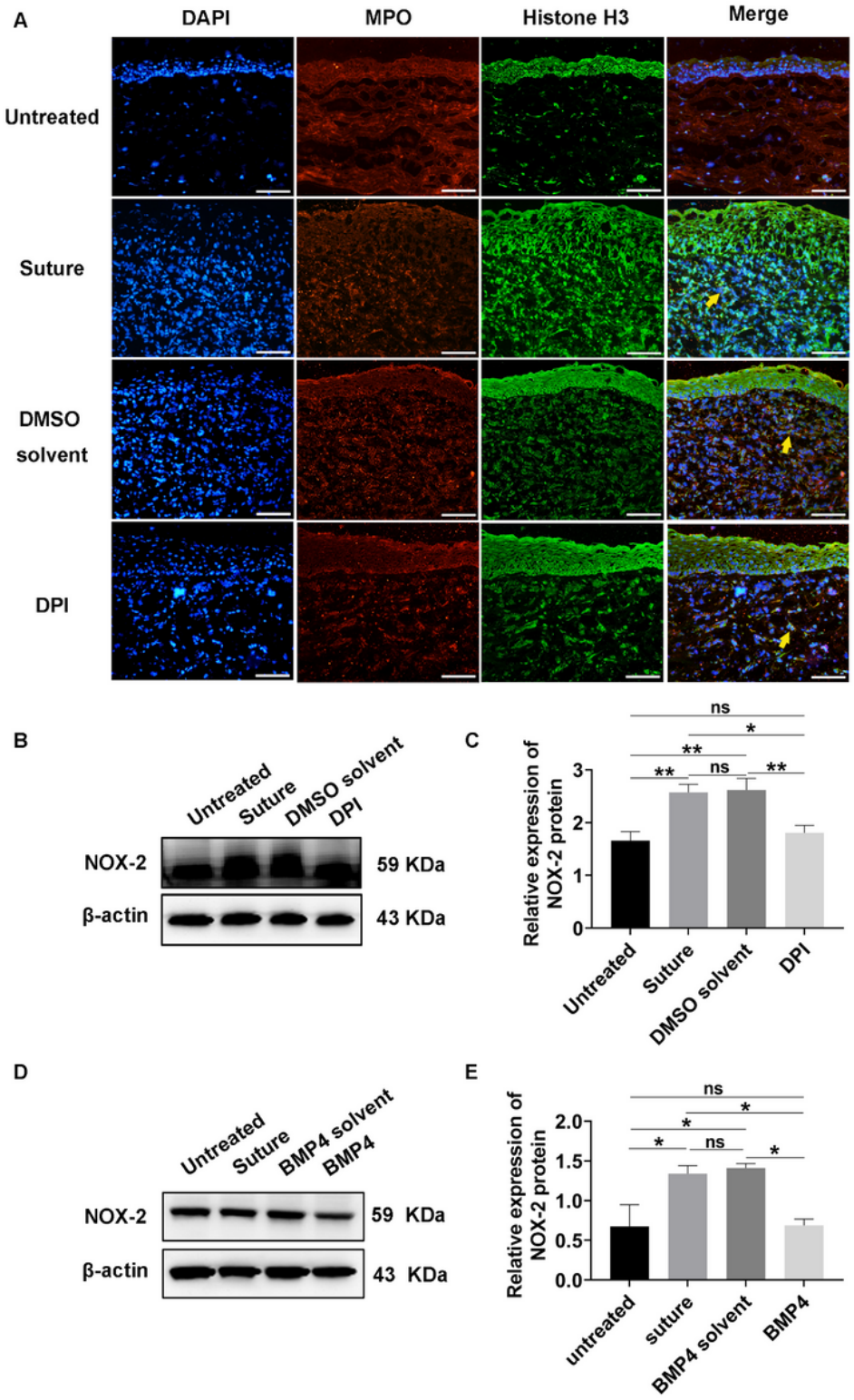

Figure 8

Effect of diphenyleneiodonium chloride (DPI) on NETs formation in the suture-induced CNV model. (A) Immunofluorescence staining showed that DPI reduced the formation of NETs. (B) Protein expression levels of NOX-2 in the DPI group, DMSO control group, suture group and the untreated group were accessed using western blot analysis on day 7. (C) Quantitative analysis of NOX-2 protein density in the DPI group, DMSO control group, suture group and the untreated group. (D) The protein level of Nox-2 in

the BMP4 group was examined by western blot analysis. (E) Quantitative analysis of NOX-2 protein density in the BMP4 group, solvent control group, suture group and the untreated group . Results are presented as means±SEM. *P <0.05. **P<0.01. (n=6).

Supplementary Files

This is a list of supplementary files associated with this preprint. Click to download.

- GA.png